ADSORPTION OF PIPERAZINE-DITHIOCARBAMATE ON Au(111): AN ELECTROCHEMICAL SCANNING TUNNELING MICROSCOPY STUDY

ADSORCIÓN DE PIPERAZINA-DITIOCARBAMATO EN Au(111): ESTUDIO MEDIANTE MICROSCOPÍA DE BARRIDO POR EFECTO TÚNEL ELECTROQUÍMICO

M. P. Hernández[a*], J. A. Martínez[a†], G. Navarro-Marín[b], J. Valenzuela[c], J. A. Herrera[a], M. H. Farías[c]

a) Instituto de Ciencia y Tecnología de Materiales (IMRE), Universidad de La Habana, La Habana 10400, Cuba; javmar@imre.uh.cu†
b) Department of Physics, University of Basel, 4056 Basel, Switzerland
c) Centro de Nanociencias y Nanotecnología (CNyN), Universidad Nacional Autónoma de México (UNAM), Ensenada, BC, 22860, Mexico
† corresponding author

Recibido 28/1/2026; Aceptado 2/6/2026

* *In memoriam*

The adsorption process of piperazine-dithiocarbamate potassium salt, which occurs on the Au(111) surface, was studied by using electrochemical scanning tunneling microscopy. Perchloric acid and sodium hydroxide were used as electrolytes. The results revealed that, depending on the applied potential and the nature of the electrolyte, the entire molecule or just individual sulfur atoms were adsorbed forming different sulfur phases, instead of the entire molecule.

Mediante el empleo de la microscopía de barrido por efecto túnel en ambiente electroquímico, se estudió el proceso de adsorción de la sal ditiocarbamato-piperazina de potasio sobre la superficie de Au(111). Se emplearon ácido perclórico e hidróxido de sodio como electrólitos. Los resultados mostraron que, en dependencia del potencial aplicado y la naturaleza del electrólito, se produjo la adsorción de la molécula completa, o solamente de sus átomos de azufre, formando diferentes tipos de estructuras.

Keywords: Thin films, scanning tunneling microscopy, electrochemistry, microscopy of surfaces, interfaces.

I. INTRODUCTION

Dithiocarbamate is a sulfur-based functional group, and their compounds are employed as building blocks for self-assembled monolayers (SAMs) on gold surfaces. These SAMs can be easily prepared in liquid phase by deposition from solutions because of the high affinity between sulfur and gold atoms, with applications as electrochemical sensors and in the preparation of molecular devices [1–6]. Under certain conditions during the deposition process, only sulfur atoms are adsorbed on gold, by the breaking of the bond between sulfur and the rest of the molecule [7–11]. Under different conditions the entire molecule is adsorbed on the surface, thus forming SAMs [12, 13]. This behavior is strongly related to the chemical and physical properties of the dithiocarbamate solution (concentration, pH, temperature) [14–16].

Some aspects of the interaction between sulfur and gold have not been completely explained yet, like the adsorbate mobility [17], the ordering of atoms forming different structures or phases [18–21], the presence of vacancies or holes in the surface [21–23], the lifting of the surface reconstruction, the adsorption mechanism [17–25], and the surface sites where it takes place [21, 26–28]. By using electrochemical scanning tunneling microscopy (EC-STM) [29], the influence of the electrical potentials and pH in the processes of adsorption/desorption of the molecules or atoms on the surface can be studied in real time, together with the structure formation and surface modifications.

Dithiocarbamate adsorption has been previously studied by experimental techniques like X-ray photoelectron spectroscopy (XPS) [3, 6, 8], atomic force microscopy (AFM) and scanning tunneling microscopy (STM) [3, 7, 8, 11–13], but not by EC-STM. In this article, we used EC-STM for studying the behavior of the piperazine-dithiocarbamate of potassium molecules (K_2DTC_2pz) in solution, interacting with a polycrystalline Au(111) surface in acid (perchloric acid, $HClO_4$) and basic (sodium hydroxide, NaOH) environments.

II. EXPERIMENTAL

Starting materials: Potassium and sodium hydroxides (Alfa Aesar, p.a. quality); piperazine, perchloric acid, methanol, and carbon disulfide (Merck, p.a.). K_2DTC_2pz was synthesized as follows: 1 g of KOH was added to a solution containing 5 ML of methanol and 3 ML of CS_2. This solution was stirred until the KOH was completely dissolved, and then 194.2 mg of piperazine were added. The resulting solution was reacted for 30–40 min, and afterwards, it was rotoevaporated until completely dried [7].

In situ STM images were taken at 298 K with a Digital Instruments Nanoscope E electrochemical scanning tunneling microscope (EC-STM) equipped with a bi-potentiostat, using tungsten tips, etched from a polycrystalline wire in aqueous NaOH. The tips were polymer coated to reduce the faradaic current at the tip-electrolyte interface. All images were recorded in the constant current mode, and processed with

the WSxM software [30].

The EC-STM electrochemical cell consists of an Au(111) polycrystalline thin film on a borosilicate substrate with an area of $12 \times 12\,mm^2$ (Arrandee^{TM}) as a working electrode (WE), two platinum wires served as counter and reference electrodes. The reported potentials (E) are in the saturated calomel electrode (SCE) scale ($E_{Pt} - E_{SCE} = 0.55\,V$) [31]. Before each experiment, the Au WE was annealed in a hydrogen flame for about 3 min and cooled down to room temperature. Samples were first immersed at open circuit potential (ocp) in aqueous 0.004 mM K_2DTC_2pz in 0.5 M NaOH or $HClO_4$. The samples were imaged in the most intense electro-reduction/oxidation peaks. Imaging potentials ranged from - 1.4 to 0.5 V.

III. RESULTS AND DISCUSSION

Figure 1 shows the EC-STM images of an Au(111) surface immersed in the K_2DTC_2pz solution in basic medium obtained at two different electrochemical potentials. At $E = -0.825\,V$ (Figure 1a), totally covered terraces by quasi-ordered structures were observed, composed of bright spots in rectangular-like arrays (region 1). At more positive potentials ($E = -0.790\,V$, Figure 1b), the coverage on the surface breaks with the order observed in Figure 1a. This image shows three different height features: small regions with several bright spots corresponding to atoms or arrays of atoms with different structures (region 2, 3, 4); a zone widely covered by a layer of adsorbate with no apparent order (5); and a few darker zones (6), corresponding to etch pits of the surface.

Figure 2a shows a closer inspection of region 1 of the modified gold surface, revealing more details of the rectangular-like arrangement, with well-ordered spots. This structure is formed by parallel chains of spots in either I and II directions, having intercalated bright and dark spots forming hexamer-like structures. The length of the chains is $(1.16 \pm 0.02)\,nm$, the distance between the atoms in the chains is $(0.59 \pm 0.06)\,nm$, and the separation between them is $(0.55 \pm 0.03)\,nm$, as shown in profiles I and II (Figure 2 b and c). Taking into account that the heights in the profiles have an average value of $(0.16 \pm 0.03)\,nm$, they might correspond to sulfur atoms from the molecule. This can be explained, considering that due to the presence of the gold surface, a strong interaction is established between the sulfur and gold atoms, yielding the adsorption of sulfur and breaking of sulfur-carbon bonds, leaving the rest of the dithiocarbamate molecule in the electrolyte solution.

Assuming a non-reconstructed Au(111) surface, this hexamer-like pattern can be described with a $\begin{pmatrix} 4 & 0 \\ 1 & \sqrt{3} \end{pmatrix}$ structure with an approximate coverage of 0.25 ML.

A zoom area of the squared region 2 from Figure 1b (Figure 3) presented several brilliant spots forming regular patterns composed of four atoms (tetramers). From the height profiles, similar to those of the previous case, we concluded that these tetramers structures were composed only of sulfur atoms, with dimensions $(0.56 \pm 0.08) \times (0.63 \pm 0.08)\,nm$. A comparison with the dimensions of the sulfur tetramers previously observed on Au(100) by STM ($0.57 \times 0.56\,nm$) [7] reveals that the tetramers observed under electrochemical conditions in the basic environment on this surface are smaller than the ones observed in air on Au(100). Assuming again that there was no Au(111) reconstruction, this phase can be described with a $\begin{pmatrix} 2 & 0 \\ \sqrt{5}/2 & \sqrt{15}/2 \end{pmatrix}$ structure, that corresponds to a coverage of 0.2 ML. A zoom of region 3 in Figure 1b appears in Figure 4. This region also presents the sulfur atoms arranged in a quasi-rectangular array of dimensions $(1.54 \pm 0.08) \times (0.68 \pm 0.08)nm$ in two orientations, being its structure $\begin{pmatrix} \frac{9}{2} & \frac{3\sqrt{3}}{2} \\ \frac{5}{2} & \frac{5\sqrt{3}}{4} \end{pmatrix}$, that corresponds to a very dilute coverage of 0.07 ML.

Region 4 also from Figure 1b was also magnified (Figure 5) to reveal very bright spots without any kind of order. The height of these spots is about $(0.28 \pm 0.03)\,nm$, remarkably higher than the heights observed for the previously studied cases. We attributed these spots to the whole molecule anchored to the surface with a tilt of about 60°, which should explain why these points have a higher height.

The coexistence of several arrangements of sulfur atoms and the presence of K_2DTC_2pz molecules in Figure 1b demonstrates that at this potential the system has a very dynamical behavior, being that all the sulfur atoms are not completely separated from the molecules, and not in their most stable arrangement on the Au surface, resulting in a coexistence of molecules and different arrangements of atoms.

In the case of perchloric acid as an electrolyte, at a potential $E = -0.447\,V$, an oblique-shaped array covering wide areas of the surface appears (Figure 6). From the profile, we can establish that the separation between the spots has a mean value of $(0.41 \pm 0.02) \times (0.35 \pm 0.05)\,nm$, and the crystallographic angles have an average value of $(65 \pm 1)°$ and $(115 \pm 2)°$. This structure can be mathematically described by a $\begin{pmatrix} \sqrt{2} & 0 \\ \frac{3}{5} & \frac{3\sqrt{3}}{5} \end{pmatrix}$ structure. The heights of the peaks in Figure 6, with an average value of $(0.25 \pm 0.03)\,nm$, are similar than those present in Figure 5; therefore, this structure should be formed only by tilted molecules. Then, we can associate each bright spot with the K_2DTC_2pz molecule, adsorbed over the Au(111) surface, forming a SAM with the afore mentioned structure, corresponding to a dense coverage of 0.75 ML.

Increasing E yields desorption of the sulfur atoms, disappearing the ordered structure, as was observed at $E = +103\,mV$ (Figure 7). The figure shows a diluted phase, where the spots corresponding to the sulfur atoms appear extended, indicating their mobility over the surface before desorption, which is completely reached at higher potentials.

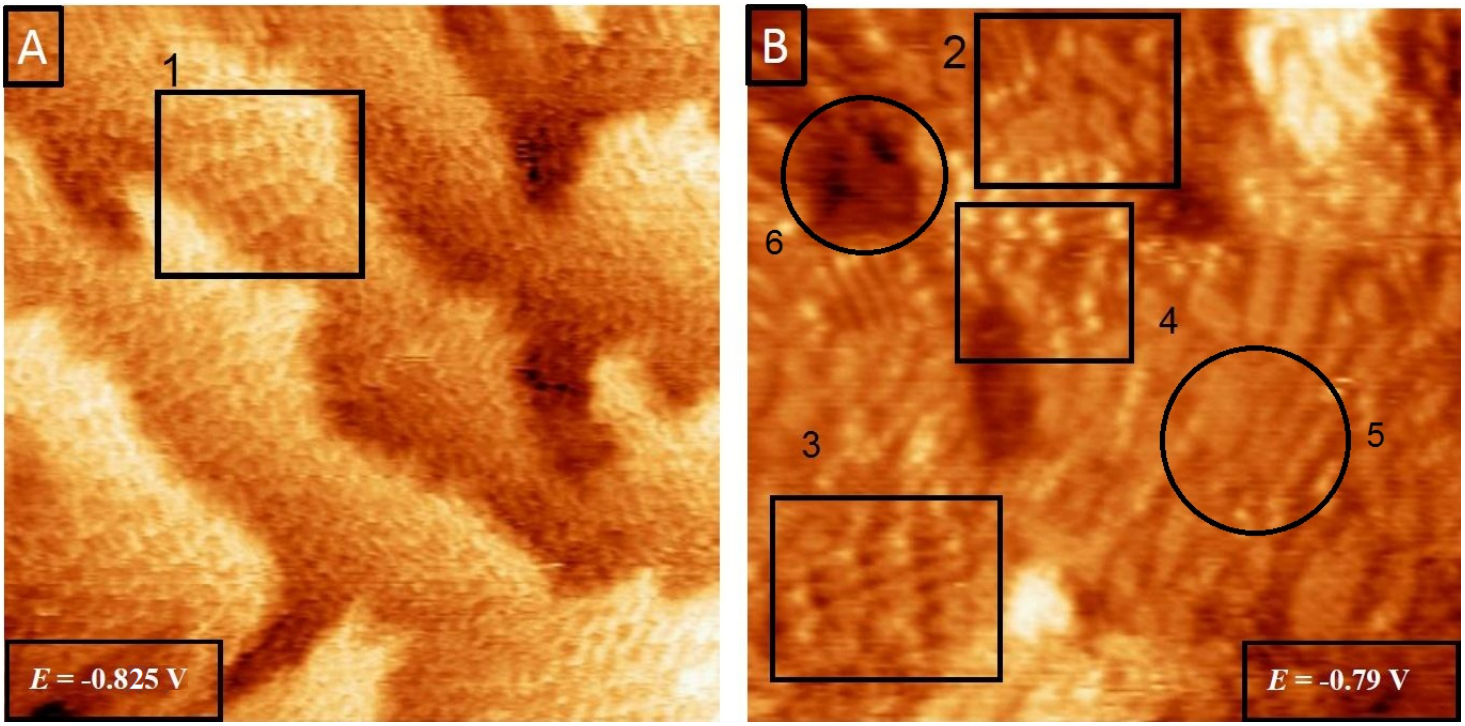

Figure 1. a) Unfiltered EC-STM image of $15.4 \times 15.5\,\mathrm{nm}^2$ of the Au(111) surface modified with K_2DTC_2pz in 0.5 M KOH: b) $E = -0.825\,\mathrm{V}$, $V_{bias} = -64\,\mathrm{mV}$, $I = 6\,\mathrm{nA}$, $f = 5.8\,\mathrm{Hz}$; b) $E = -0.790\,\mathrm{V}$, $V_{bias} = -49\,\mathrm{mV}$, $I = 5.4\,\mathrm{nA}$, $f = 8.1\,\mathrm{Hz}$.

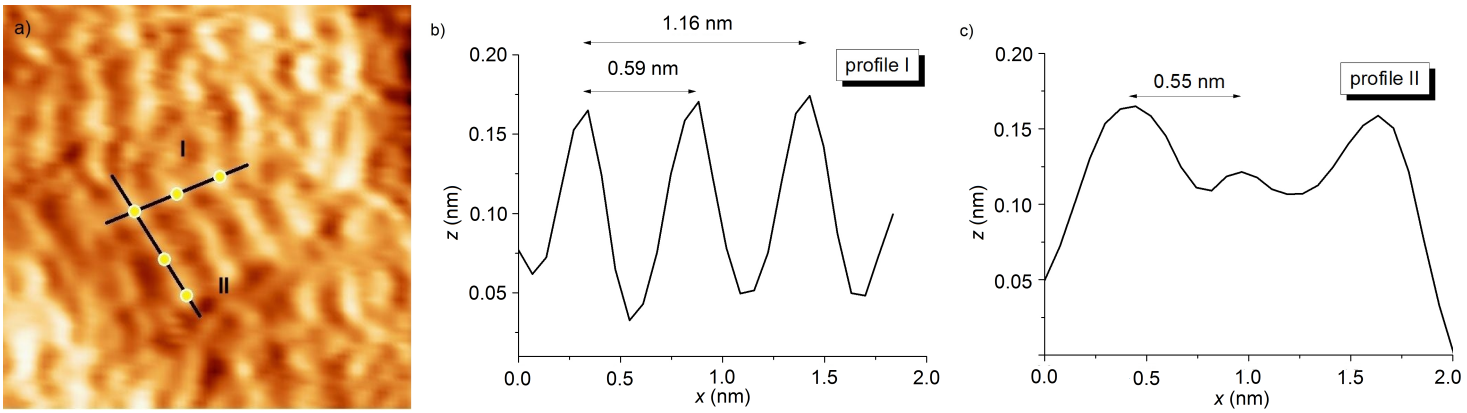

Figure 2. Unfiltered ECSTM image $4.7 \times 4.4\,\mathrm{nm}^2$ from region inside box 1 on Figure 1a, showing rectangular patterns formed by six atoms. Line profiles I and II correspond to directions I and II (Figure 2b and c). Yellow circles mark the sulfur atoms.

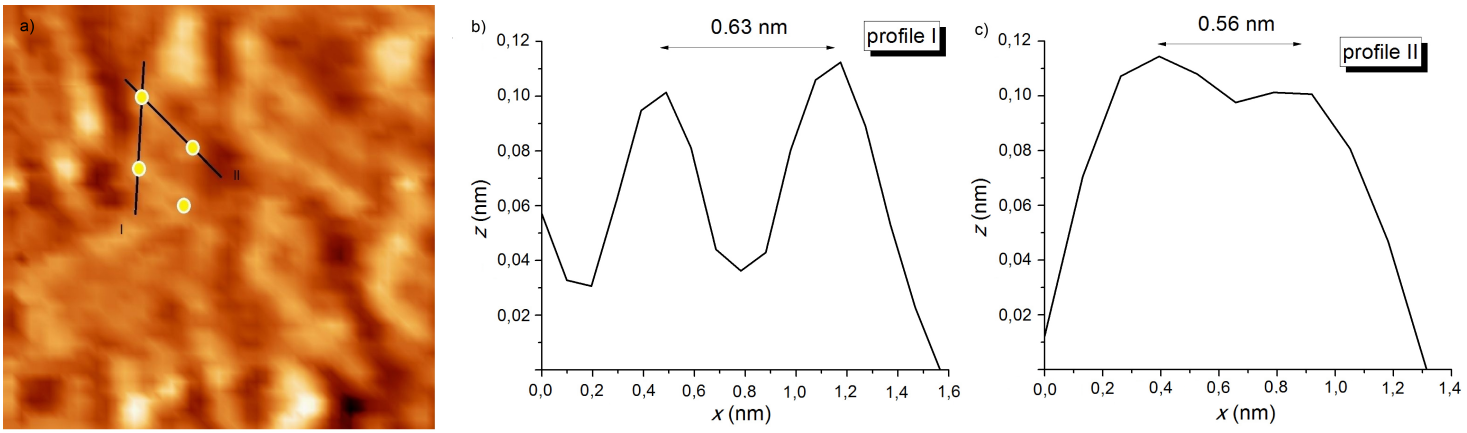

Figure 3. Unfiltered ECSTM image $4.7 \times 4.4\,\mathrm{nm}^2$ from region inside box 2 on Figure 1b showing tetramers. Line profiles I and II correspond to directions I and II (Figure 3b and c). Yellow circles mark the sulfur atoms.

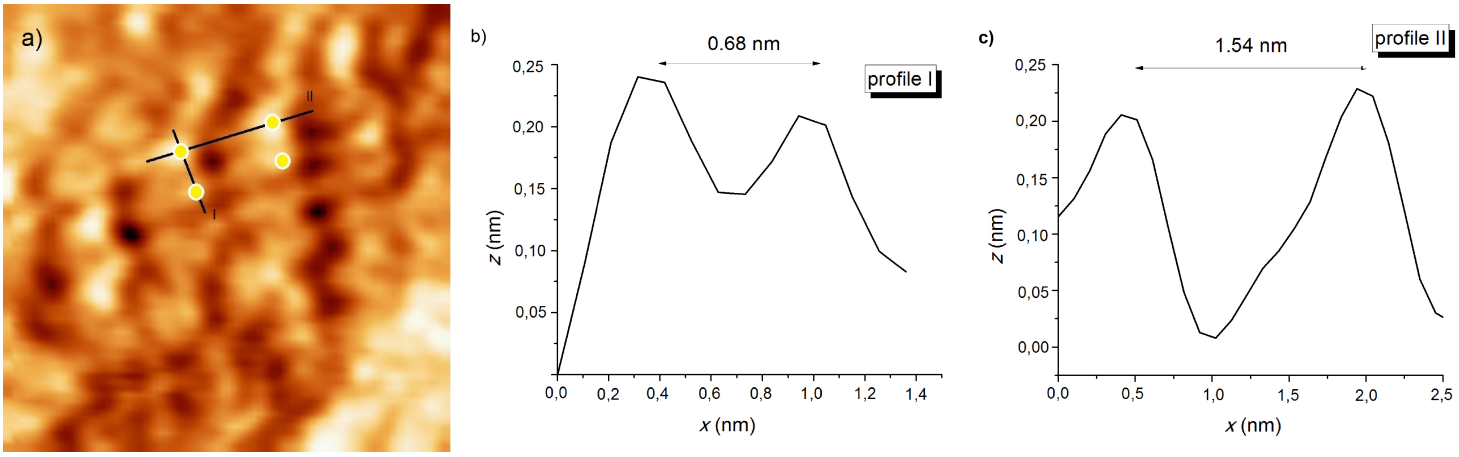

Figure 4. ECSTM image $7 \times 7\,\mathrm{nm}^2$ from region inside box 3 on Figure 1b showing a quasi-rectangular array. Line profiles I and II correspond to directions I and II (Figure 4b and c). Yellow circles mark the sulfur atoms.

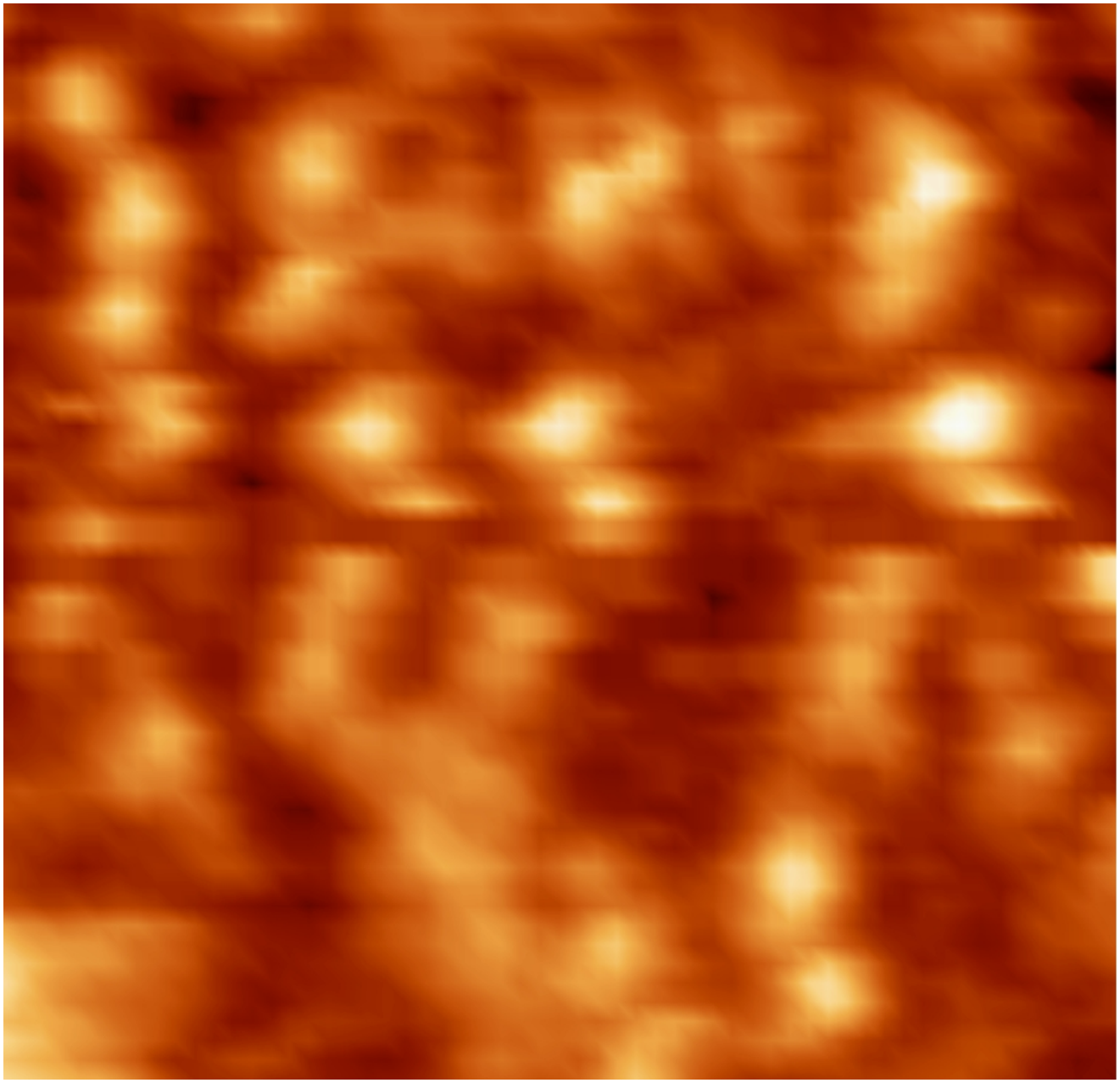

Figure 5. EC-STM image $6 \times 6\,\mathrm{nm}^2$ of region 4 of Figure 1b showing very bright spots.

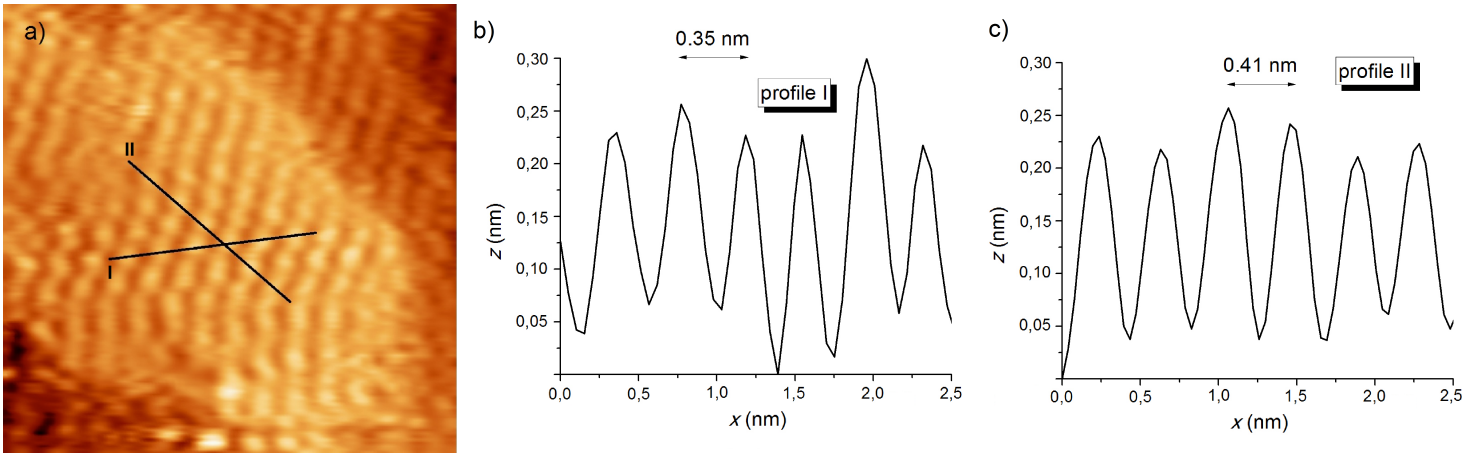

Figure 6. Unfiltered ECSTM image of $6 \times 6\,\mathrm{nm}^2$ of the Au(111) modified with K_2DTC_2pz in 0.5 M HClO4: a) $E = -0.447\,\mathrm{V}$, $V_{bias} = -144\,\mathrm{mV}$, $I = 24\,\mathrm{nA}$, $f = 5.8\,\mathrm{Hz}$. Line profiles I and II correspond to directions I and II (Figure 6b and c).

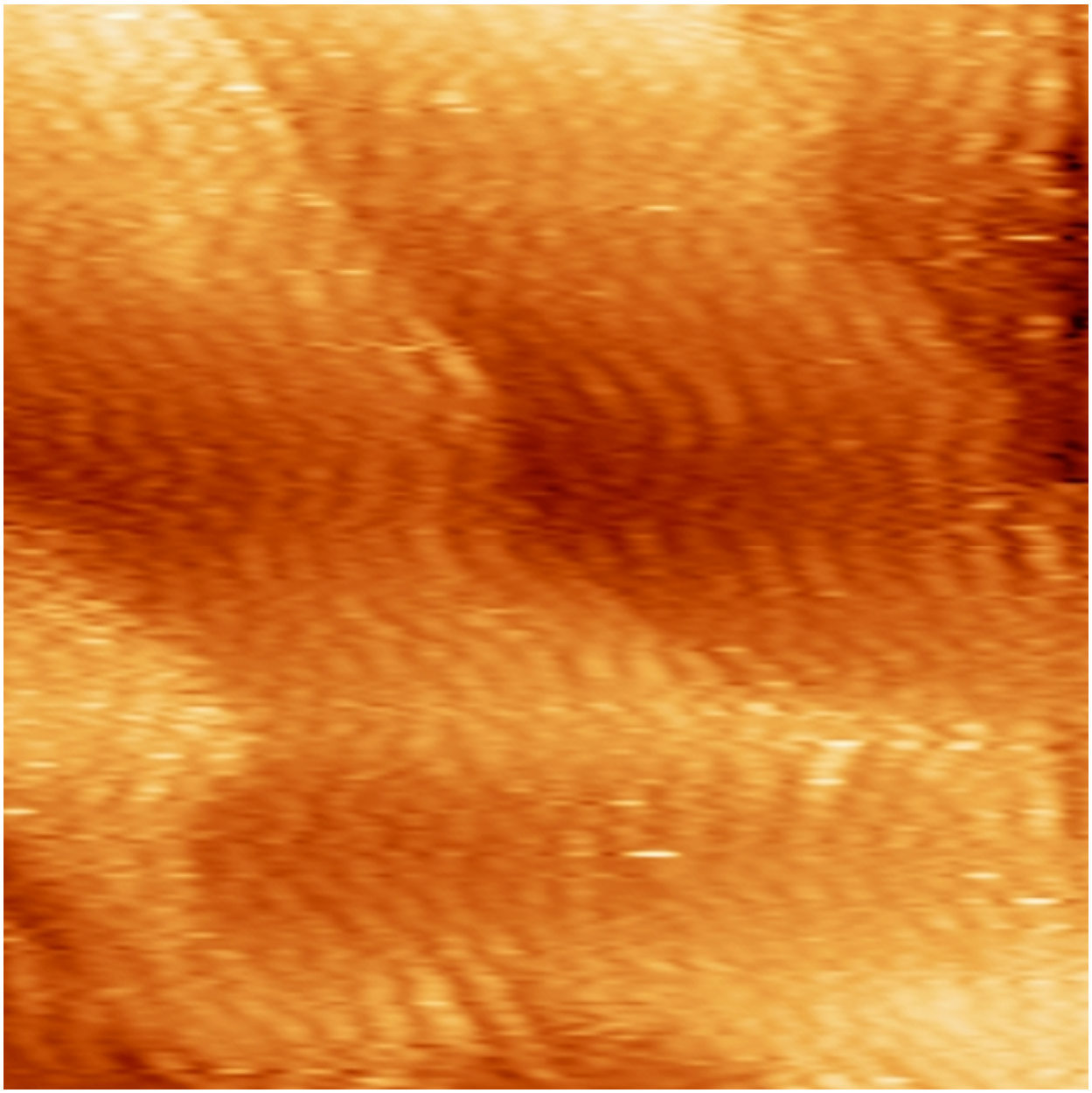

Figure 7. Unfiltered EC-STM image of $10 \times 10\,\mathrm{nm}^2$ of the Au(111) modified with K_2DTC_2pz in 0.5 M HClO4: a) $E = 103\,\mathrm{mV}$, $V_{bias} = -144\,\mathrm{mV}$, $I = 24\,\mathrm{nA}$, $f = 3.9\,\mathrm{Hz}$.

IV. CONCLUSIONS

The different structures formed by means of the adsorption of dithiocarbamates are studied by electrochemical scanning tunneling microscopy for the first time. These experiments were carried out taking into account the changes in the chemical environment (acid or basic) and the applied potential.

The presence of two different kinds of electrolytes brings us the opportunity to study the influence of chemical conditions on the adsorption of the piperazine-dithiocarbamate molecules. In both cases, depending on the potentials applied, we observed different features in the adsorbed layers: SAMs of sulfur atoms, more or less ordered, or without any ordered structures; and entire molecules of piperazine-dithiocarbamate. The resulting features are strongly dependent on the electrochemical environment and the applied potentials, dealing with the adsorption of the entire molecule or only sulfur atoms.

The presence, under certain conditions, of the entire molecule is remarkable because it allows us the possibility to study the electrochemical conditions to get the adsorption of individual sulfur atoms or the molecule, to resolve one of the most intriguing aspects of the dithiocarbamates adsorption: the conditions determining when the single sulfur atoms or the entire molecules are adsorbed.

V. ACKNOWLEDGEMENT

This work was supported by a joint grant from Centro Latinoamericano de Física and The Abdus Salam International Centre for Theoretical Physics (CLAF-ICTP) awarded to Javier A. Martínez. We appreciate the support provided by Proyecto Nacional de Ciencias Básicas (PNCB) Code: PN223LH010-045. [12, 13]

REFERENCES

[1] W. E. Ford, D. Gao, F. Scholz, G. Nelles, F. von Wrochem, *Chem. Mater.*, **25**, 3603–3613 (2013).

[2] W. E. Ford, D. Gao, F. Scholz, G. Nelles, F. von Wrochem, *ACS Nano*, **7**, 1943–1951 (2013).

[3] D. Gao, F. Scholz, H.-G. Nothofer, W. Ford, U. Scherf, J. M. Wessels, A. Yasuda, F. von Wrochem, *J. Am. Chem. Soc.*, **133**, 5921–5930 (2011).

[4] Z. Li, M. Smeu, T. H. Park, J. Rawson, Y. Xing, M. J. Therien, M. A. Ratner, E. Borguet, *Nano Lett.*, **14**, 5493–5499 (2014).

[5] F. von Wrochem, D. Gao, H.-G. Nothofer, G. Nelles, J. M. Wessels, *Nat. Nanotechnol.*, **5**, 618–624 (2010).

[6] D. Meyer, T. Schäfer, P. Schulz, S. Jung, J. Rittich, D. Mokros, I. Segger, F. Maercks, C. Effertz, R. Mazzarello, M. Wuttig, *Langmuir*, **32**, 8812–8817 (2016).

[7] J. A. Martínez, J. Valenzuela B., R. Cao Milán, J. Herrera, M. H. Farías, M. P. Hernández, *Appl. Surf. Sci.*, **320**, 287–293 (2014).

[8] J. A. Martínez, J. Valenzuela, C. E. Hernández-Tamargo, R. Cao–Milán, J. A. Herrera, J. A. Díaz, M. H. Farías, H. Mikosch, M. P. Hernández, *Appl. Surf. Sci.*, **345**, 394–399 (2015).

[9] C. E. Hernández-Tamargo, R. Barzaga, H. Mikosch, J. A. Martínez, J. A. Herrera, M. H. Farías, M. P. Hernández, *Phys. Chem. Chem. Phys.*, **18**, 29987–29998 (2016).

[10] C. E. Hernández-Tamargo, A. L. Montero-Alejo, D. Codorníu Pujals, H. Mikosch, M. P. Hernández, *J. Chem. Phys.*, **141**, 044713-1–10 (2014).

[11] R. Barzaga, J. A. Martínez, M. H. Farías, M. P. Hernández, *J. Phys. Chem. C*, **123**, 12183–12194 (2019).

[12] A. F. Raigoza, G. Kolettis, D. A. Villalba, S. A. Kandel, *J. Phys. Chem. C*, **115**, 20274–20281 (2011).

[13] P. Morf, N. Ballav, M. Putero, F. von Wrochem, J. M. Wessels, T. A. Jung, *J. Phys. Chem. Lett.*, **1**, 813–816 (2010).

[14] J. C. Love, L. A. Estroff, J. K. Kriebel, R. G. Nuzzo, G. M. Whitesides, *Chem. Rev.*, **105**, 1103–1169 (2005).

[15] R. G. Nuzzo, D. L. Allara, *J. Am. Chem. Soc.*, **105**, 4481–4483 (1983).

[16] A. H. A. Mamun, J. R. Hahn, *Surf. Sci.*, **606**, 664–669 (2012).

[17] K. M. Koczkur, E. M. Hamed, A. Houmam, *Langmuir*, **27**, 12270–12274 (2011).

[18] A. Houmam, K. M. Koczkur, G. Moula, E. M. Hamed, *ChemPhysChem*, **13**, 1240–1245 (2012).

[19] A. Houmam, H. Muhammad, K. M. Koczkur, *Langmuir*, **28**, 16881–16889 (2012).

[20] C. Schlaup, D. Friebel, P. Broekmann, K. Wandelt, *Surf. Sci.*, **602**, 864–870 (2008).

[21] C. Vericat, M. E. Vela, J. Gago, R. C. Salvarezza, *Electrochim. Acta*, **49**, 3643–3649 (2004).

[22] M. M. Biener, J. Biener, C. M. Friend, *Langmuir*, **21**, 1668 (2005).

[23] M. Biener, J. Biener, C. M. Friend, *Surf. Sci.*, **601**, 1659–1667 (2007).

[24] M. E. Vela, H. Martin, C. Vericat, G. Andreasen, A. Hernández Creus, R. C. Salvarezza, *J. Phys. Chem. B*, **104**, 11878–11882 (2000).

[25] H. Walen, D.-J. Liu, J. Oh, H. J. Yang, Y. Kim, P. A. Thiel, *J. Phys. Chem. C*, **119**, 21000–21017 (2015).

[26] P. G. Lustemberg, C. Vericat, G. A. Benítez, M. E. Vela, N. Tognalli, A. Fainstein, M. L. Martiarena, R. C. Salvarezza, *J. Phys. Chem. C*, **112**, 11394–11402 (2008).

[27] S. Y. Quek, M. M. Biener, J. Biener, J. Bhattacharjee, C. M. Friend, U. V. Waghmare, E. Kaxiras, *J. Phys. Chem. B*, **110**, 15663–15665 (2006).

[28] C. Vericat, G. Andreasen, M. E. Vela, R. C. Salvarezza, *J. Phys. Chem. B*, **104**, 302–307 (2000).

[29] R. Wiesendanger, *Scanning Probe Microscopy and Spectroscopy*, Cambridge University Press, 1994, pp. 283–284.

[30] I. Horcas, R. Fernández, J. M. Gómez-Rodríguez, J. Colchero, J. Gómez-Herrero, A. M. Baró, *Rev. Sci. Instrum.*, **78**, 013705 (2007).

[31] A. Cuesta, M. Kleinert, D. M. Kolb, *Phys. Chem. Chem. Phys.*, **2**, 5684–5690 (2000).